

β A3/A1-Crystallin controls anoikis-mediated cell death in astrocytes by modulating PI3K/AKT/mTOR and ERK survival pathways through the PKD/Bit1-signaling axis

B Ma^{1,2,3}, T Sen^{1,3}, L Asnaghi¹, M Valapala¹, F Yang¹, S Hose¹, DS McLeod¹, Y Lu², C Eberhart¹, JS Zigler Jr¹ and D Sinha^{*,1}

During eye development, apoptosis is vital to the maturation of highly specialized structures such as the lens and retina. Several forms of apoptosis have been described, including anoikis, a form of apoptosis triggered by inadequate or inappropriate cell–matrix contacts. The anoikis regulators, Bit1 (Bcl-2 inhibitor of transcription-1) and protein kinase-D (PKD), are expressed in developing lens when the organelles are present in lens fibers, but are downregulated as active denucleation is initiated. We have previously shown that in rats with a spontaneous mutation in the *Cryba1* gene, coding for β A3/A1-crystallin, normal denucleation of lens fibers is inhibited. In rats with this mutation (*Nuc1*), both Bit1 and PKD remain abnormally high in lens fiber cells. To determine whether β A3/A1-crystallin has a role in anoikis, we induced anoikis *in vitro* and conducted mechanistic studies on astrocytes, cells known to express β A3/A1-crystallin. The expression pattern of Bit1 in retina correlates temporally with the development of astrocytes. Our data also indicate that loss of β A3/A1-crystallin in astrocytes results in a failure of Bit1 to be trafficked to the Golgi, thereby suppressing anoikis. This loss of β A3/A1-crystallin also induces insulin-like growth factor-II, which increases cell survival and growth by modulating the phosphatidylinositol-3-kinase (PI3K)/AKT/mTOR and extracellular signal-regulated kinase pathways. We propose that β A3/A1-crystallin is a novel regulator of both life and death decisions in ocular astrocytes. *Cell Death and Disease* (2011) 2, e217; doi:10.1038/cddis.2011.100; published online 13 October 2011

Subject Category: Neuroscience

The eye has provided crucial insights into the processes and mechanisms of development, from tissue induction to the apoptosis-mediated remodeling required for maturation of highly specialized structures such as the lens and retina.^{1–4} Apoptosis has a crucial role during development, tissue homeostasis and disease. Several forms of apoptosis have been described, including anoikis, which is initiated by loss of cell anchorage.^{5,6} Two proteins, Bit1 (Bcl-2 inhibitor of transcription-1) and its upstream regulator, protein kinase-D, or protein kinase-D (PKD), have been shown to control anoikis.⁷ Bit1 was reported as a mitochondrial protein that promotes caspase-independent apoptosis when released into the cytoplasm.⁸ However, a recent study has shown that Bit1 localizes to the early secretory pathway in the endoplasmic reticulum (ER) microdomains and is enriched in the Golgi complex.⁹ The apoptotic function of Bit1 is inhibited by integrin-mediated cell attachment.⁷

It has been suggested that several pathways could contribute to protection of cells from anoikis.^{10,11} Bit1 negatively regulates the extracellular signal-regulated kinase (ERK) mitogen-activated protein kinase (MAPK) survival

pathway.¹² Phosphatidylinositol-3-kinase (PI3K)/AKT/mTOR (mammalian target of rapamycin) has been postulated to mediate anoikis-suppressing effects in cells.¹² Interestingly, a macrophage-stimulating protein has been shown to protect epithelial cells from cell death through both the ERK and PI3K/AKT pathways.¹³ Several growth factors, for example insulin-like growth factor-II (IGF-II), are also known to activate cell survival pathways that promote proliferation and inhibit apoptosis.¹⁴ The precursor form of IGF-II (proIGF-II), but not mature IGF-II (mIGF-II), is a potent activator of the PI3K/Akt and ERK signaling cascades.¹⁵

In the eye, programmed removal of nuclei and other organelles from lens fiber cells is essential to remove light-scattering centers and provide an optically clear path to the retina. Denucleation in normally differentiating lens fiber cells involves many of the cellular and molecular events of apoptosis.^{16–18} However, although lens fiber cells lose their organelles, as in apoptosis, they do not die; rather, they remain viable throughout life. The mechanisms involved in this apoptosis-like process in the lens remain largely unknown. We have shown that a spontaneous mutation (*Nuc1*) in the

¹The Wilmer Eye Institute, The Johns Hopkins University School of Medicine, Baltimore, MD, USA and ²Department of Ophthalmology, Eye and ENT Hospital of Fudan University, Shanghai, China

*Corresponding author: D Sinha, The Wilmer Eye Institute—Ophthalmology, The Johns Hopkins University School of Medicine, Baltimore, MD 21287, USA.

Tel: +410-502-2100; Fax: +410-614-6728; E-mail: Debasish@jhmi.edu

³These authors contributed equally to this work.

Keywords: anoikis; astrocytes; β A3/A1-crystallin; lens denucleation; PI3K/AKT/mTOR and ERK pathways

Abbreviations: AIF, apoptosis-inducing factor; Bit1, Bcl-2 inhibitor of transcription-1; BSA, bovine serum albumin; E, embryonic day; ER, endoplasmic reticulum; ERK, extracellular signal-regulated kinase; GFAP, glial fibrillary acidic protein; IGF-II, insulin-like growth factor-II; ILK, integrin-linked kinase; MAPK, mitogen-activated protein kinase; mIGF-II, mature IGF-II; M-PER, Mammalian Protein Extraction Reagent; MTS, 3-(4,5-dimethylthiazol-2-yl)-5-(3-carboxymethoxyphenyl)-2-(4-sulfophenyl)-2H-tetrazolium; P, postnatal day; PBS, phosphate-buffered saline; PFV, persistent fetal vasculature disease; PI3K, phosphatidylinositol-3-kinase; PKD, protein kinase-D; poly-HEMA, poly-2-hydroxyethyl methacrylate; proIGF-II, precursor form of IGF-II; siRNA, small interfering RNA; TTBS, Tris-buffered saline; wt, wild type

Received 26.5.11; revised 25.8.11; accepted 12.9.11; Edited by A Verkhratsky

Cryba1 gene, coding for β A3/A1-crystallin, an abundant structural protein of lens fibers,^{19,20} inhibits normal denucleation of lens fibers.²¹ Like other crystallins, β A3/A1-crystallin is also expressed outside of the lens and probably has a role beyond that of a structural protein. We have shown earlier that in the neural retina, β A3/A1-crystallin is expressed by astrocytes.²² We have also provided novel evidence, based on our studies using Nuc1 rat, that this protein has a pivotal role in the migration, proliferation and patterning of retinal astrocytes.^{22,23}

Astrocytes are one of the two glial cell types found in the retina. Several studies have shown that all types of retinal neurons and the Muller glial cells descend from a common progenitor.^{24,25} However, astrocytes originate outside of the retina, arising from the neuroepithelial cells that form the optic stalk, the primordium of the optic nerve.²⁶ They migrate from the optic nerve into the inner retina, increasing in number until 6 weeks after birth.^{27,28} It has been shown that during postnatal development of the rat optic nerve 50% of oligodendrocytes normally die, but no astrocyte death was observed.²⁷ Moreover, in the early postnatal rat cerebellum, a majority of astrocytes are eliminated as a mechanism to adjust their numbers to the needs of the tissue.²⁹ It is possible that during development astrocyte cell numbers are controlled by a different apoptotic process than all other retinal cell types. Our previous studies suggest that astrocytes have a pivotal role in the remodeling of the retina; therefore, maintaining a proper astrocyte cell number is critical.²²

We report here that both Bit1 and PKD are differentially expressed in lens during the denucleation process. However, in Nuc1 homozygous lenses, where the mutation inhibits normal denucleation of lens fibers, expression of both Bit1 and PKD remain abnormally high. These data prompted us to investigate a possible role for β A3/A1-crystallin in anoikis-mediated cell death. As we have reported earlier that astrocytes in the neural retina express β A3/A1-crystallin and regulate the remodeling of the retina, we investigated the possibility that astrocyte cell numbers might be regulated by anoikis.

We propose that β A3/A1-crystallin is required by astrocytes for trafficking of Bit1 to the Golgi, which is essential for anoikis-mediated cell death. Our data also indicate that loss of β A3/A1-crystallin induces IGF-II and increases cell survival by regulating the PI3K/AKT/mTOR and ERK pathways, thereby protecting astrocytes from anoikis-mediated cell death.

Results

Expression pattern of Bit1 during lens denucleation. To test our hypothesis that anoikis is involved in lens denucleation, we compared immunofluorescent staining for Bit1 in lenses from wild-type (wt) and Nuc1 homozygous rats ranging from E (embryonic day) 14.5 to P (postnatal day) 10 (Figure 1). At E14.5, when the posterior epithelial cells of the lens vesicle are elongating to form primary fibers, there is weak staining for Bit1, primarily in the fibers, in both genotypes. At E17.5, when the primary fiber cells have filled the lens vesicle, both wt and Nuc1 lenses were strongly positive for Bit1 in fibers and epithelial cells. At E19.5 in the

wt lens, secondary fibers in the bow region, as well as central primary fibers, were positive for Bit1, as was the lens epithelium; in Nuc1 lenses, Bit1 was seen throughout the disorganized lens. By P3, the wt lenses lose Bit1 expression in the central fiber cells, with weak expression remaining in the younger, peripheral fiber cells. At P10, staining at the periphery was further decreased in the wt lens, with only epithelial cells and fibers in the bow region being positive. By contrast, staining in Nuc1 lenses at P3 and P10 remained strong throughout the lens.

PKD expression pattern during lens denucleation. To determine whether PKD, the upstream regulator of Bit1, was expressed in lens, and whether expression correlated with denucleation, frozen sections of lenses from the same stages as above were examined by immunofluorescence. Interestingly, we found that PKD staining showed a similar pattern to Bit1 in the wt lens except that epithelial cells were negative (Figure 2A). Specifically, PKD was expressed in primary fiber cells by E14.5. By E19.5, PKD was expressed throughout the lens fiber mass, similarly in wt and Nuc1 lenses. PKD expression in the wt lens started to decrease by P3 and was clearly downregulated by P10. However, as with Bit1, PKD expression was sustained in Nuc1 lens both at P3 and P10. Western blot analysis confirmed that PKD protein decreased in wt lens at P3 and P10, whereas no such decrease occurred in Nuc1 (Figure 2B).

Bit1 expression in optic nerve and retinal astrocytes. We have shown previously that β A3/A1-crystallin is expressed in the wt neural retina and the optic nerve. Expression of the anoikis regulators, Bit1 and PKD, has not been shown previously in the retina, or in astrocytes. In the rat optic nerve, Bit1 expression was evident by E19 (Figure 3A, a); by P3, Bit1 and glial fibrillary acidic protein (GFAP) were strongly co-expressed, indicating that mature astrocytes express Bit1 (Figure 3A, d–f). Interestingly, at P10, GFAP⁺ optic nerve astrocytes no longer express Bit1 (Figure 3A, g–j). Bit1 expression in postnatal retina showed a similar pattern. Retinal flat mounts from wt rats showed that GFAP⁺ astrocytes (green) also expressed Bit1 (red) at P3 (Figure 3B, a–c). However, by P10 the expression of Bit1 (red) shifted from astrocytes (green) to probably Muller cells (Figure 3B, d–f). Astrocytes migrate from the optic nerve into the inner retina and increase in number until 6 weeks after birth. Our data show that at 2 months of age, Bit1 was expressed in the wt optic nerve, co-expressing with GFAP⁺ astrocytes (Figures 4a–c). In the neural retina, however, Bit1 does not co-express strongly with GFAP; rather, it appears to be expressed predominantly by Muller glial cells (Figures 4d–f). We have reported earlier that the Nuc1 mutation affects programmed cell death, and we find much stronger co-expression of Bit1 with GFAP in the Nuc1 retina (Figures 4j–l, arrows in panel l show co-expression). The pattern of Bit1 expression in Nuc1 optic nerve is similar to wt (Figures 4g–i). We also show that in primary cultures of wt astrocytes, Bit1 colocalizes with giantin, a Golgi marker (Figures 5a–c). In Nuc1 astrocytes, however, Bit1 shows minimal colocalization with giantin (Figures 5d–f), suggesting failure of Bit1 trafficking. It has been reported that Bit1 localizes to the

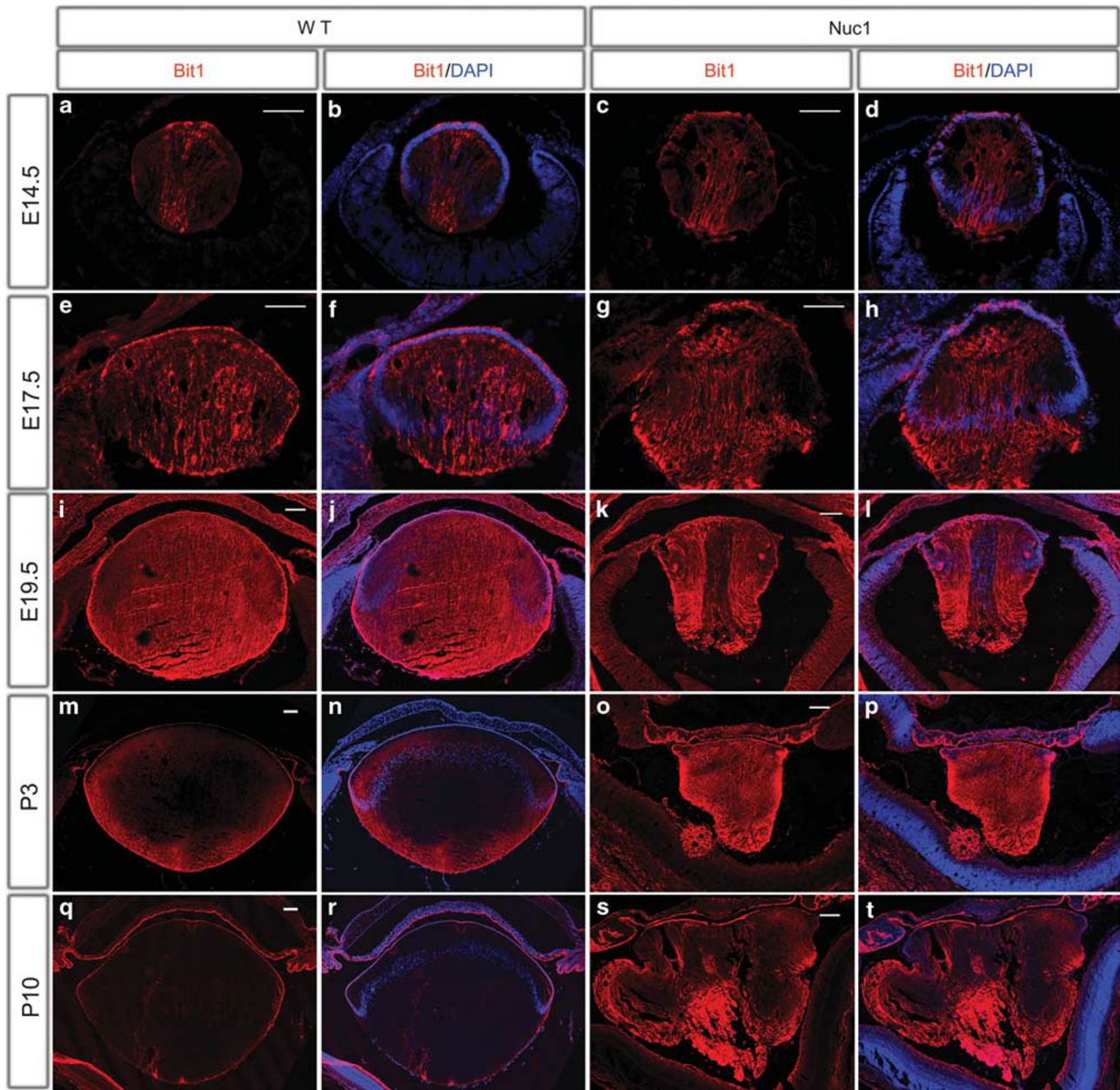


Figure 1 Immunofluorescent labeling of Bit1 was performed on frozen sections of wt and Nuc1 homozygous lenses aged E14.5 to P10. At E14.5, Bit1 staining (red) was visible in the elongating primary fibers and in the lens epithelial cells in both genotypes (a–d). When primary fiber cells have filled the lens vesicle at E17.5 (e–h), both wt and Nuc1 lens fibers and epithelial cells were positive for Bit1, with similar pattern at E19.5 (i–l). By P3 (m–p), the central fiber cells started losing their Bit1 staining. By contrast, Nuc1 mutants showed positive staining for Bit1 from E19.5 to P3, with abnormal retention of nuclei. By P10 (q–t), Bit1 staining in the fibers declined further in the wt lenses and positive staining was seen only in the epithelium and bow region. The Bit1 staining pattern of Nuc1 lenses remained strong both in the fibers and epithelium. Nuclei were counterstained with DAPI where indicated. Scale bar = 50 μ m

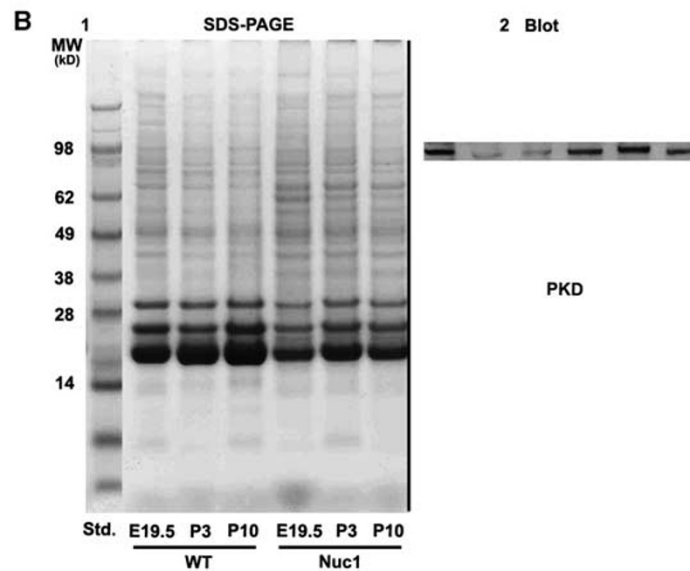
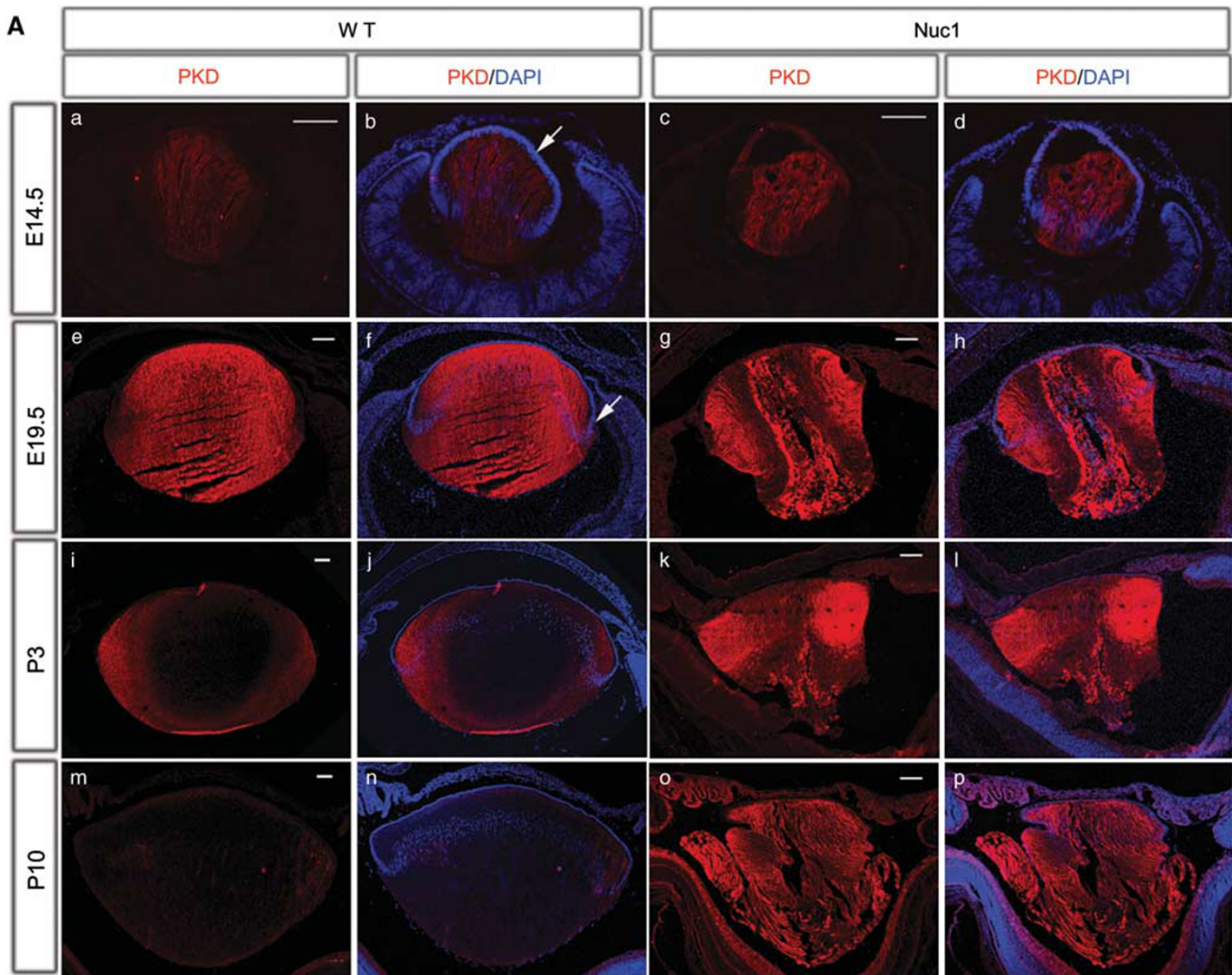
early secretory pathway and is enriched in the Golgi, and that localization in the Golgi is important for anoikis-mediated cell death.⁹ These data further prompted us to use astrocytes to investigate a possible role for β A3/A1-crystallin in anoikis.

β A3/A1-Crystallin and anoikis-mediated cell death in astrocytes. Anoikis was induced in astrocytes isolated from P2 wt and Nuc1 optic nerves by growing the cells in plates coated with poly-2-hydroxyethyl methacrylate (poly-HEMA)

to prevent adhesion to the substrate. After 5 days in culture, we observed only small and sparse aggregates of cells in the wt cultures, whereas Nuc1 cultures showed larger and more numerous cellular aggregates (Figure 6a). After 3 days of anoikis induction, cell death was 20% greater in wt cultures than in Nuc1; by 5 days, cell death in wt cultures was > 2-fold higher than in Nuc1 cultures (Figure 6b). Moreover, MTS (3-(4,5-dimethylthiazol-2-yl)-5-(3-carboxymethoxyphenyl)-2-(4-sulfophenyl)-2H-tetrazolium) assays conducted after 5

days of anoikis induction (poly-HEMA) followed by 7 days in normal culture conditions demonstrated increased proliferation by Nuc1 cells (Figure 6c). Western blot data

indicated that total PKD protein and phosphorylated PKD are higher in Nuc1 astrocytes as compared with wt. However, no difference in the protein levels of Bit1, cleaved caspase-3 or



apoptosis-inducing factor (AIF) was seen between wt and Nuc1 astrocytes (Figure 6d). To confirm its role in anoikis-mediated cell death in astrocytes, we knocked down Bit1 in wt astrocyte using a Bit1-specific small interfering RNA (siRNA). Our data show decreased cell death after anoikis induction in astrocytes where Bit1 is downregulated (Figure 6e).

Loss of β A3/A1-crystallin inhibits anoikis-mediated cell death and increases cell survival by modulating the PI3K/Akt/mTOR and ERK pathways. The PI3K/AKT/mTOR and p44/42 MAPK (ERK1/2) pathways are known to promote cell survival. Our data show that in Nuc1 astrocytes, phosphorylated PI3K, AKT and mTOR are upregulated as compared with wt after 3 and 5 days of anoikis induction (Figure 7a). We also found that phosphorylated ERK1/2 protein expression is increased in Nuc1 astrocytes, relative to wt cells, after anoikis induction (Figure 7a). Whereas ERK1/2 total protein was equivalent in wt and Nuc1 astrocytes after anoikis induction, total PI3K and AKT protein were increased in Nuc1 astrocytes as compared with wt (Figure 7a). Moreover, the phosphorylated form of integrin-linked kinase (ILK) was also increased in Nuc1 astrocytes as compared with wt after 3 and 5 days of anoikis induction, whereas total ILK remained unchanged (Figure 7a).

To determine whether survival of Nuc1 astrocytes is regulated by the mTOR and ERK1/2 pathways, we treated wt and Nuc1 astrocytes for 72 h with either rapamycin (10 nM), an inhibitor of mTOR, or the ERK inhibitor FR180204 (10 μ M). Results showed a decrease in the proliferation of the Nuc1 astrocytes after treatment with either FR180204 or rapamycin (Figure 7b). Interestingly, the presence of both inhibitors had a stronger effect than either applied alone, indicating an additive effect when both pathways were inhibited (Figure 7b). Moreover, when wt and Nuc1 astrocytes were exposed to FR180204, rapamycin or both under an anoikis condition, a remarkable increase in cell death was observed in Nuc1 astrocytes but not in wt cells (Figure 7c).

IGF-II expression levels in optic nerve astrocytes. To identify growth factors that might be responsible for upregulation of survival pathways in Nuc1 astrocytes, we evaluated microarray data comparing wt and Nuc1 astrocytes from both the optic nerve and retina (data not shown). A striking increase in IGF-II was observed in Nuc1 cells. This result was confirmed by quantitative real-time PCR analysis performed on 2- and 7-day cultures of optic nerve astrocytes. As shown in Figure 8a, increases of about 27-fold (2 day) and 73-fold (7 day) were observed in the Nuc1 astrocytes as compared with wt when normalized to the

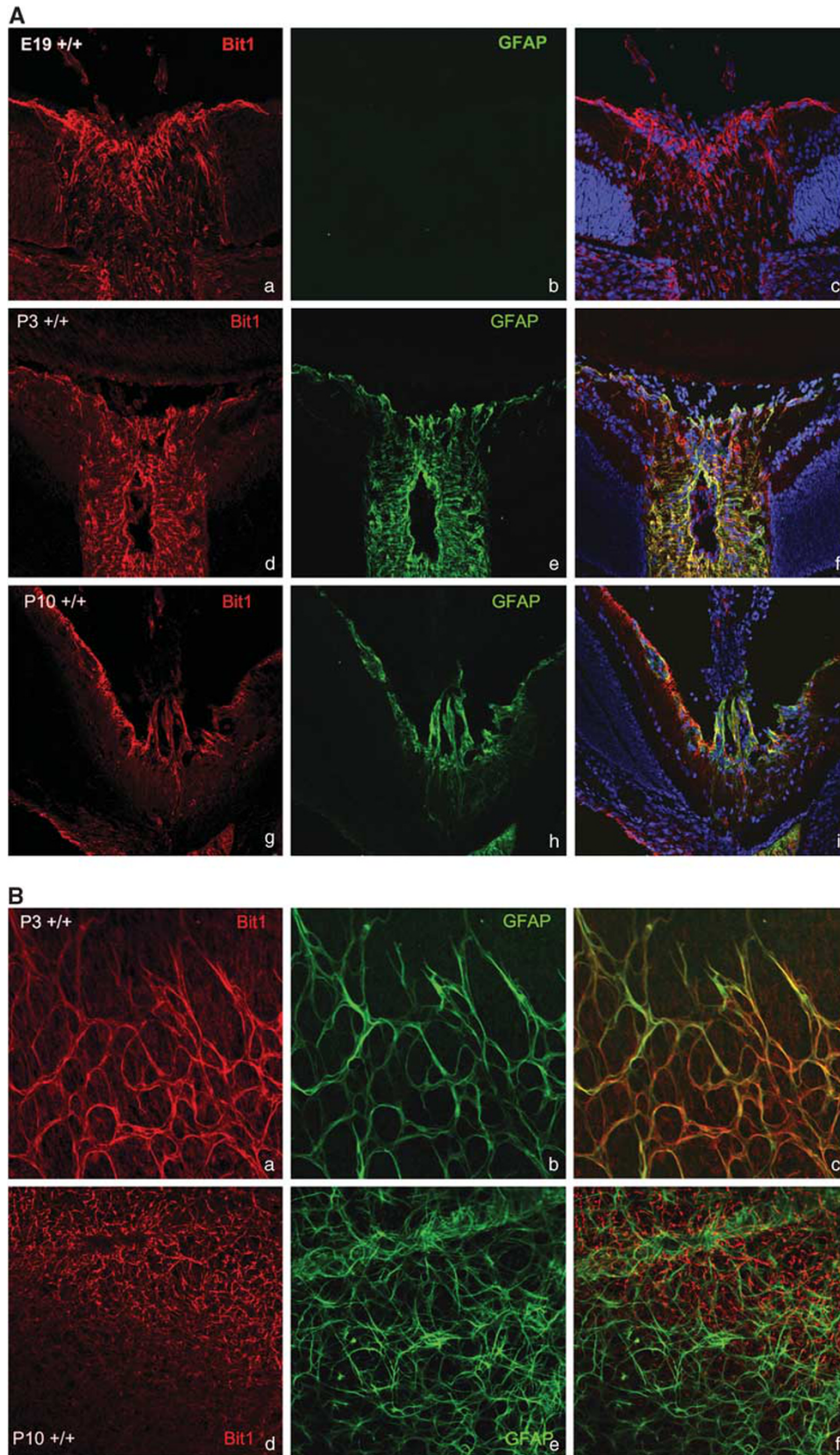
reference gene, *Gapdh*. Western blot analysis also showed markedly higher levels of proIGF-II in Nuc1 astrocytes as compared with wt (Figure 8b).

Discussion

We have hypothesized previously, based on our studies using the Nuc1 rat model, that β A3/A1-crystallin may have a role in programmed cell death during ocular development.^{21,22,30,31} Nuc1 rats have a complex ocular phenotype, including nuclear cataracts, persistent fetal vasculature disease (PFV) and abnormalities in retinal vasculature development.^{21–23,30,31} β A3/A1-crystallin, a member of the β/γ -crystallin superfamily, is abundantly expressed in differentiating lens fiber cells. Programmed removal of nuclei and other organelles from lens fiber cells occurs as elongating lens fiber cells detach from the capsule and later inter-digitate with apposing fibers to form sutures.³² Anoikis is a form of apoptosis resulting from loss of cell anchorage.³³ To determine whether anoikis is involved in denucleation of lens fiber cells, we evaluated the expression patterns of the anoikis regulators, Bit1 and PKD, in the developing rat lens. Our studies show that expression of both Bit1 and PKD is modulated during the process of lens denucleation (Figures 1 and 2). In wt lens, Bit1 and PKD are highly expressed during embryonic development, when the organelles are still present in lens fibers, but are down-regulated as active denucleation is initiated. Interestingly, in Nuc1 rat, where a mutation in the *Cryba1* gene inhibits normal programmed loss of nuclei, expression of both Bit1 and PKD remains abnormally high in mature lens fibers. These data suggest that anoikis may be involved in the lens denucleation process. To determine whether β A3/A1-crystallin has a role in anoikis, we induced anoikis *in vitro* and conducted mechanistic studies on astrocytes, cells known to express β A3/A1-crystallin.

Astrocytes are the only cells in the retina that are immigrants to the retina, and their numbers appear to be controlled by a different cell death process than that functioning in those cell types that are born in the retina.^{34,35} Programmed cell death of astrocytes in the rat retina peaks between P0 and P5, and declines by P15.³⁶ Interestingly, the anoikis effectors, Bit1 and PKD, are also expressed in the developing retina. Our data indicate that in the wt optic nerve and developing retina, Bit1 is expressed as early as E19 (Figure 3). By P3 Bit1 is expressed by GFAP⁺ astrocytes. Astrocytes first appear in the developing rat optic nerve at E16, but they are immature and do not express GFAP. By P3 they become GFAP⁺ (Figure 3). They form a corona of processes around the optic nerve head by E18, cover approximately 35% of the retina at birth and reach the periphery of the retina by P8.³⁶ Thus, the expression pattern of Bit1 correlates temporally with the development of astrocytes, suggesting a role for anoikis-mediated cell death

Figure 2 (A) Photomicrographs of wt and Nuc1 lenses immuno-labeled for PKD (red), an upstream regulator of Bit1. PKD has a staining pattern similar to that of Bit1, except that lens epithelial cells (arrows) were negative for PKD. Immunostaining showed weak expression of PKD in lens primary fibers at E14.5 both in wt and Nuc1 lenses (a–d). There was no marked difference in PKD expression between wt and Nuc1 through E19.5 (a–h). At P3 (i–l) PKD staining was diminished in the wt lens, but not in Nuc1, from the mature fiber cells in the core. By P10 (m–p), only fiber cells at the equatorial area expressed PKD. In Nuc1, PKD staining was present throughout the disorganized lens at both P3 and P10. Nuclei were counterstained with DAPI. (B) Western blot analysis showed that PKD protein is expressed at E19.5 in both wt and Nuc1 homozygous lenses. However, in wt expression decreased markedly by P3 and P10, whereas PKD expression was not downregulated in the Nuc1 homozygous lenses



in the regulation of astrocyte cell numbers in the developing retina. By P10, Bit1 appears to be expressed by Muller cells (Figures 3 and 4), whereas expression by astrocytes is downregulated. This raises the interesting possibility that a

population of Muller cells may be controlled by anoikis-mediated cell death in the developing retina. However, Bit1 may also have other roles in cellular homeostasis that remain to be determined.

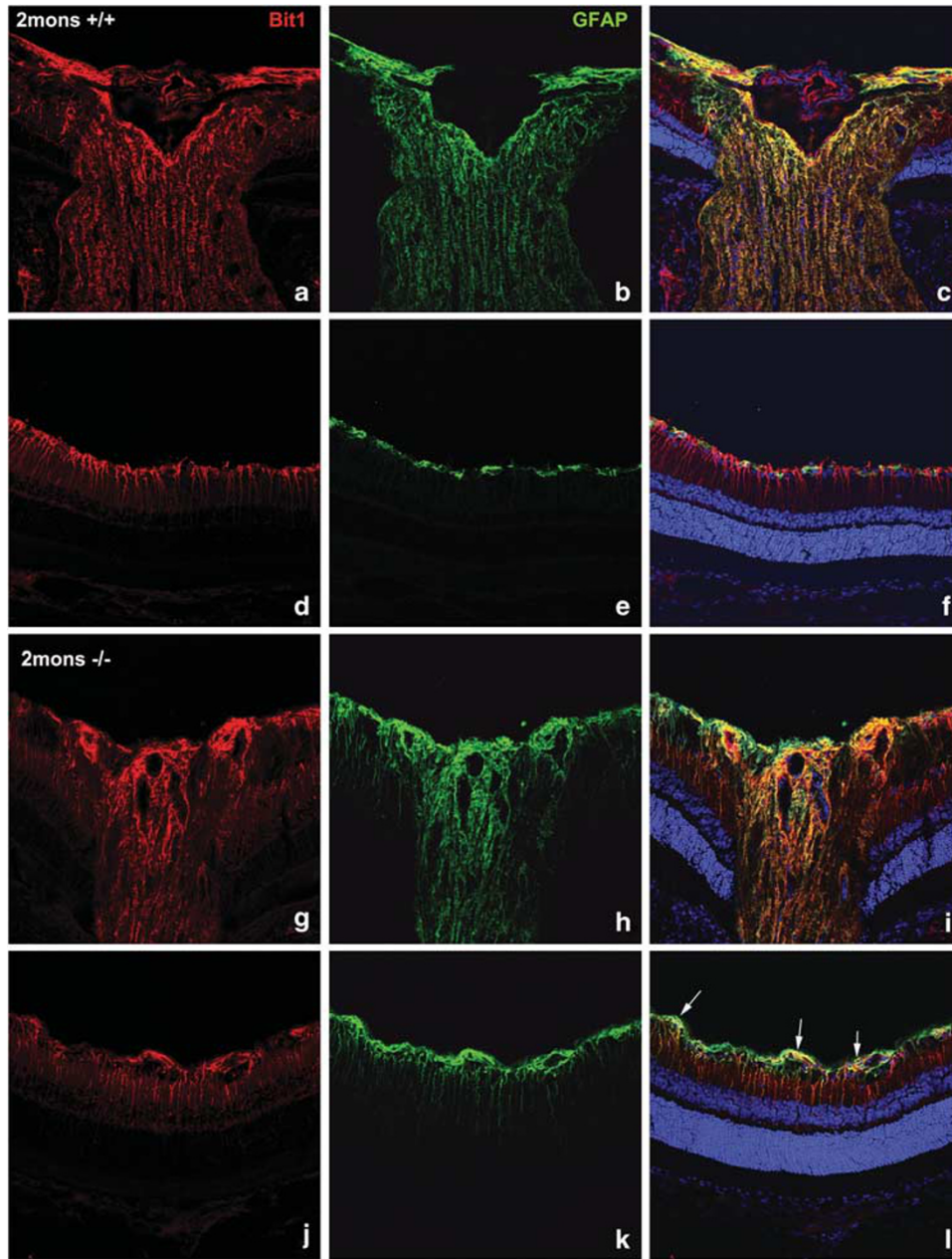


Figure 4 Bit1 expression in the retina and optic nerve head in normal (a–f) and Nuc1 homozygous rats (g–l) at 2 months of age. Confocal microscopy indicated that in wt optic nerve (panels a–c), Bit1 (red) and GFAP (green) are co-expressed (yellow, c). The expression pattern of Bit1 (red) is different in the wt retina (panels d–f), where Bit1 expression appears to be primarily in Muller cells (d), with little co-expression with GFAP⁺ astrocytes. Interestingly, in the Nuc1 homozygous optic nerve (panels g–i) and especially in the retina (panels j–l) Bit1 (red) and GFAP (green) show greater co-expression than in wt

Figure 3 Bit1 (red) and GFAP (green) expression in optic nerve and retinal astrocytes. In panel (A) (top panel), immunofluorescent labeling of Bit1 (a) was evident in cells at the optic nerve head as early as E19. GFAP expression was not seen (b) because only immature astrocytes are present at this age. By P3 (A, middle panel), GFAP⁺ astrocytes (e) express Bit1 (d) in the optic nerve as seen in the merged image (yellow, f). However, at P10 (A, bottom panel), Bit1 (g) co-expression with GFAP was much reduced (h) in the optic nerve head (i, co-expression mostly in the nerve fiber layer of the retina). Panels c, f and i also show DAPI staining of cell nuclei (blue). Fluorescence microscopy of retinal flat mounts in panel (B), show that at P3 (top panel), Bit1 (a) and GFAP (b) are significantly co-expressed (orange, c). The Bit1 expression pattern changes by P10 (bottom panel) in the retina and GFAP⁺ astrocytes (e) no longer express Bit1 (d); expression of Bit1 now appears to be in Muller cells (f)

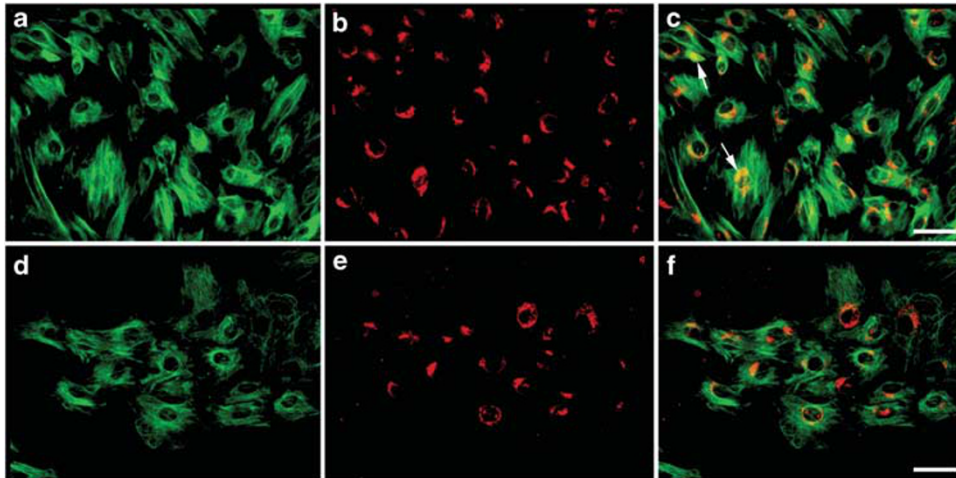


Figure 5 Fluorescence immunohistochemistry on cultured astrocytes from the optic nerve of wt (a–c) and Nuc1 homozygous rats (d–f), using antibody to Bit1 (green) and giantin (Golgi marker, red). Strong colocalization of Bit1 and giantin staining (c, arrows) is shown in the wt astrocytes. In Nuc1 astrocytes, however, Bit1 shows minimal colocalization with giantin (f). The bar represents 50 μ m

Disturbances of cell attachment are known to lead to initiation of anoikis, as demonstrated by our optic nerve astrocytes cultured on poly-HEMA plates (Figure 6a). Interestingly, anoikis-mediated cell death is reduced in Nuc1 optic nerve astrocytes cultured on poly-HEMA possibly because more cells remain attached to each other for survival (Figure 6a). These data also suggest that loss of β A3/A1-crystallin impairs anoikis in astrocytes. Cell cytotoxicity assays clearly show that the level of cell death in wt optic nerve astrocytes after anoikis induction is much higher than in Nuc1 astrocytes (Figure 6b).

Our data show increased levels of PKD in Nuc1 astrocytes after 5 days of anoikis induction, whereas protein levels of Bit1, cleaved caspase-3 and AIF are similar in wt and mutant cells under these conditions (Figure 6d). Our studies also indicate that anoikis-mediated cell death in astrocytes may occur by modulation of the Bit1–PKD axis (Figure 6e). Previous studies have indicated that Bit1 induces caspase-independent apoptosis,⁷ that it localizes to the early secretory pathway and is enriched in the Golgi.⁹ In fact, constitutive expression of Bit1 in the ER can lead to activation of the ERK–MAPK pathway and thereby inhibit anoikis.⁹ We provide evidence that, in Nuc1 astrocytes, Bit1 is not co-expressed normally with the Golgi marker giantin (Figure 5) and therefore is not enriched in the Golgi. As it has been shown that anoikis requires Bit1 trafficking to the Golgi,⁹ this may explain why Nuc1 astrocytes are able to evade anoikis even though PKD is activated. These data provide novel evidence that β A3/A1-crystallin is required by astrocytes for trafficking of Bit1 to the Golgi, which is essential for anoikis-mediated cell death. While we have no direct evidence for a role by β A3/A1-crystallin in protein trafficking, it is interesting that mutant β A3/A1-crystallin in Nuc1 fails to properly translocate to lysosomes in the retinal pigmented epithelium.³⁷

Our data suggest that loss of functional β A3/A1-crystallin not only inhibits cell death but also promotes survival of astrocytes by stimulating proliferation (Figure 6c). In cultured Nuc1 astrocytes where β A3/A1-crystallin is non-functional, the phosphorylated forms of PI3K, AKT and mTOR are

significantly increased (Figure 7a). The profound inhibition of anoikis in Nuc1 astrocytes results in the activation of survival pathways. It has been shown that activation of the PI3K/AKT/mTOR pathway may also mediate anoikis-suppressing effects in cells. It has been reported earlier that ILK is capable of phosphorylating Akt on Ser-473.³⁸ We show here that phosphorylated ILK is upregulated in Nuc1 astrocytes after anoikis induction relative to wt cells (Figure 7a), suggesting a role for ILK in anoikis-mediated cell death in astrocytes. Overexpression of ILK in mouse mammary epithelial cells (SCP2), which are anoikis-sensitive, results in profound inhibition of anoikis, whereas inhibition of ILK activity induces anoikis in human breast cancer cell lines that are normally anoikis-resistant.³⁸ ILK activity can also be triggered by growth factor stimulation in a PI3K-dependent manner.¹²

It has generally been accepted that the PI3K/AKT pathway is involved in regulation of cell survival induced by growth factors. In a recent study, it has been shown that IGF-II can activate both the PI3K/AKT and ERK pathways in ovine trophoblast cells.¹⁵ Our results raise the distinct possibility that loss of β A3/A1-crystallin can stimulate expression of IGF-II, which could regulate cell survival through the PI3K/AKT/mTOR and ERK signaling cascades. IGF-II has been shown to promote the survival of glial cells in the developing optic nerve.²⁷

To further investigate whether loss of β A3/A1-crystallin can drive cells to a survival pathway through PI3K/AKT/mTOR, we treated wt and Nuc1 astrocytes with rapamycin. Interestingly, exposing wt cells to rapamycin, an inhibitor of mTOR, did not alter cell death. However, in Nuc1 astrocyte cultures, rapamycin treatment reverses the suppressive effect of mutant β A3/A1-crystallin on anoikis (Figure 7b). Although Nuc1 astrocytes, when treated with rapamycin, underwent increased cell death, cell proliferation was still higher than that in wt astrocytes. These data suggest that a second pathway is involved in the increased survival of Nuc1 astrocytes. We therefore investigated the ERK pathway because PKD has been shown to negatively regulate ERK. In Nuc1 astrocytes, PKD is activated, however Bit1 is not trafficked to the Golgi

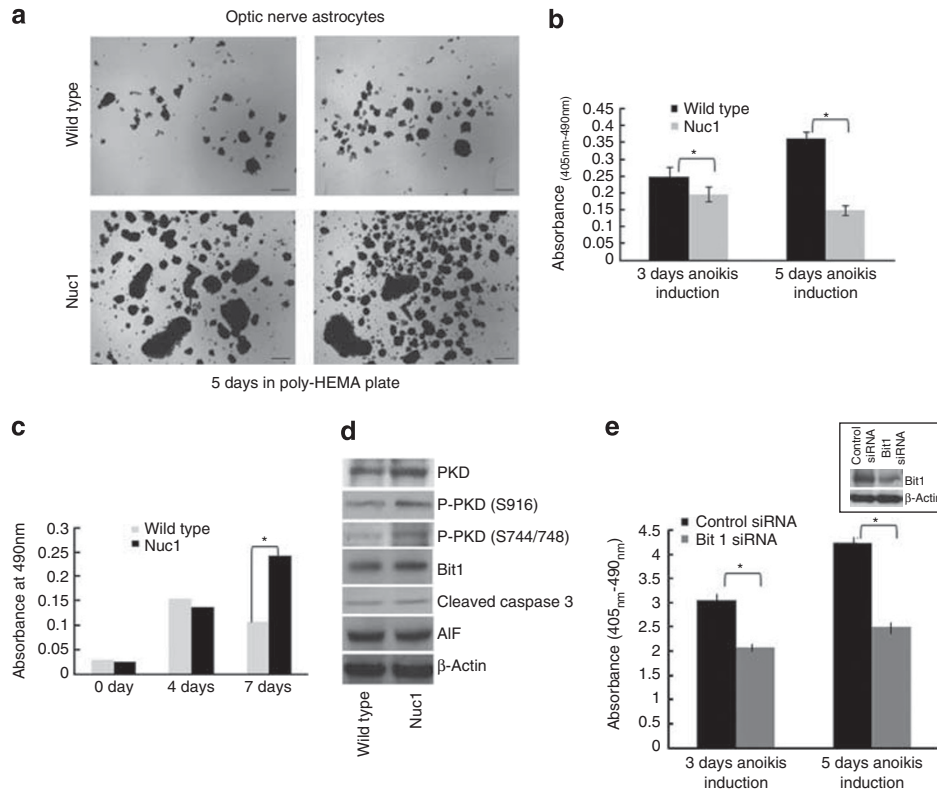


Figure 6 (a) Astrocytes were isolated from the optic nerve of wt and Nuc1 rats and cultured on poly-HEMA plates to induce anoikis. After 5 days on poly-HEMA, Nuc1 astrocytes show significantly higher survival than wt. The upper panels show representative images of wt astrocytes and the lower panels show Nuc1 cultures with larger and more numerous cellular aggregates. (b) Cell death assay performed by using the Cell Death Detection ELISA^{PLUS} kit after 3 and 5 days of anoikis induction shows, respectively, approximately 20% and 50% less cell death in Nuc1 cultures as compared with wt. Results were plotted as absorbance at 405 nm, with a reference wavelength of 490 nm. Experiments were performed in triplicate. *P*-values were calculated by Student's *t*-test ($*P = 0.001$). (c) To measure proliferation, MTS assay was performed with Nuc1 and wt astrocytes after 5 days of anoikis induction, followed by culture under normal conditions for 0, 4 and 7 days. Significant increase in cell proliferation was observed in Nuc1 cultures as compared with wt. The data represent the mean values of absorbance at wavelength 490 nm, which is proportional to the number of viable cells. Experiments were performed in triplicate. *P*-values were calculated by Student's *t*-test ($*P = 0.05$). (d) Immunoblot analyses were performed using antibodies against Bit1, PKD, phospho-PKD (Ser916 and Ser744/748), caspase-3, AIF and β -actin on lysates of wt and Nuc1 astrocytes after 3 days of anoikis induction as described under Materials and Methods. The data indicate an increase in phospho-PKD and total PKD in Nuc1 astrocytes as compared with wt. No difference in the expression patterns of Bit1, cleaved caspase-3 or AIF was seen between wt and Nuc1 astrocytes. (e) Bit1 was knocked down in wt astrocytes (western blot in inset) using a Bit1-specific siRNA as described under Materials and Methods. The data indicate that cell death was decreased in Bit1-knocked-down astrocytes after anoikis induction as described under panel a. The data represent the mean values of absorbance at wavelength 490 nm, which is proportional to the number of viable cells. Experiments were performed in triplicate. *P*-values were calculated by Student's *t*-test ($*P = 0.05$)

and therefore anoikis is suppressed. We therefore envisioned that in Nuc1 astrocytes, PKD may activate ERK as Bit1 fails to accumulate in the Golgi and the anoikis pathway is not activated. Our data do show that phosphorylated ERK1 and ERK2 are significantly increased in Nuc1 astrocytes as compared with wt after 3 and 7 days of anoikis induction, whereas total ERK protein levels remain unchanged in both wt and mutant astrocytes (Figure 7a). Moreover, treatment of Nuc1 astrocytes with the ERK inhibitor, FR180204, induced increased cell death relative to wt astrocytes. This effect was not as great as that seen with the mTOR inhibitor rapamycin. There appeared to be an additive effect on increased cell death when both inhibitors were used concomitantly, suggesting that both the PI3K/AKT/mTOR and ERK pathways are involved. Furthermore, we also show that Nuc1 astrocytes treated with the above inhibitors under an anoikis condition undergo increased cell death as compared with wt cells. We therefore provide evidence that β A3/A1-crystallin participates in cell death mechanisms essential for tissue

remodeling during ocular development by suppressing survival pathways.

In conclusion, our data provide evidence that β A3/A1-crystallin has a pivotal role in anoikis, a process necessary for tissue remodeling during eye development. Loss of this protein not only inhibits anoikis by affecting trafficking of Bit1 to the Golgi, but also activates PI3K/ERK-related survival signaling pathways, possibly through regulation of IGF-II, PKD and ILK expression (Figure 8c). Cell death during development is essential for organogenesis and crafting of complex multicellular tissues.^{39,40} In the eye, various forms of cell death occurring during development are essential for maturation of the tissue, and a defect in the process can lead to ocular diseases.

Materials and Methods

Animals. Experiments were performed using embryonic and postnatal Nuc1 and wt Sprague–Dawley rats, in accordance with the Guide for the Care and Use of Laboratory Animals (National Academy Press).

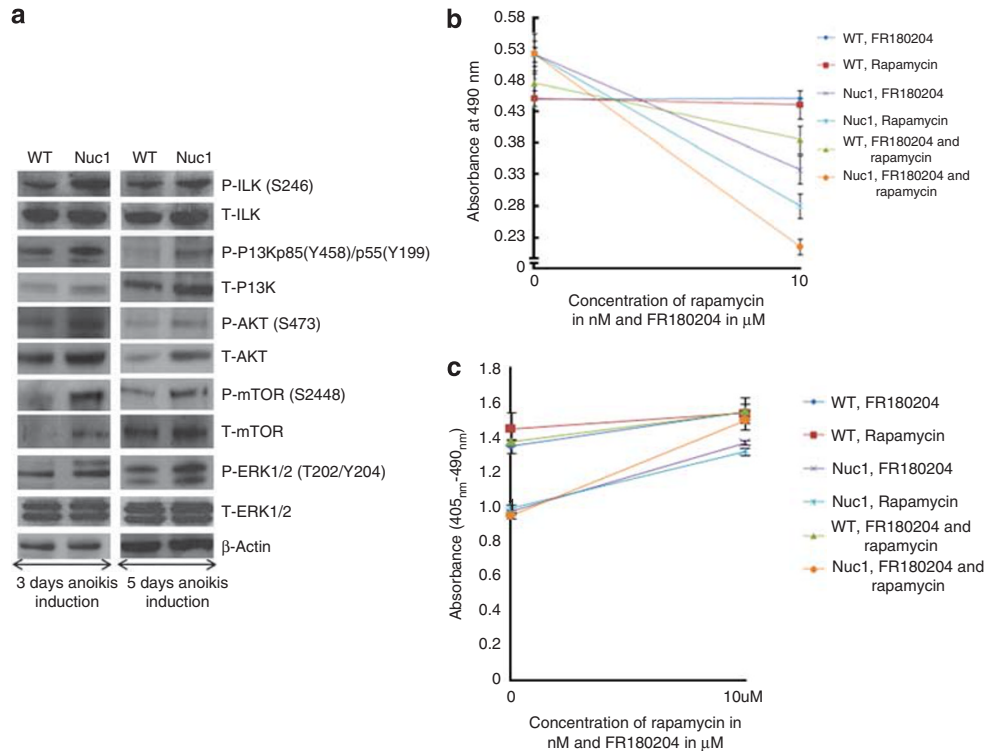


Figure 7 (a) To identify pathways activated in wt and the Nuc1 astrocytes after anoikis induction, western blot analyses were performed for total and phospho-PI3K, total and phospho-ILK, total and phospho-AKT, total and phospho-mTOR, total and phospho-ERK1/2, and β -actin. After 3 and 5 days of anoikis induction, Nuc1 astrocytes show a robust increase of phosphorylated PI3K, AKT, mTOR, ILK and ERK1/2 compared with wt. (b) MTS assays were performed after treatment of wt and Nuc1 astrocytes for 3 days with either the mTOR inhibitor, rapamycin (10 nM), or the ERK inhibitor FR180204 (10 μ M), as well as combined treatment with rapamycin (10 nM) and FR180204 (10 μ M) as described under Materials and Methods. The results show a decrease in proliferation of Nuc1 astrocytes after treatment with either rapamycin or FR180204. When both inhibitors were used together, an additive effect was observed. —◆—, wt astrocyte with FR180204 treatment; —■—, Wt astrocyte with rapamycin treatment; —▲—, wt astrocyte with rapamycin and FR180204 treatment; —×—, Nuc1 astrocyte with FR180204 treatment; —*—, Nuc1 astrocyte with rapamycin treatment; —○—, Nuc1 astrocyte with rapamycin and FR180204 treatment. (c) Cell death assays were performed on wt and Nuc1 astrocytes after culture on poly-HEMA plates for 3 days to induce anoikis and an additional 3 days (still on poly-HEMA) with either the mTOR inhibitor, rapamycin (10 nM), or the ERK inhibitor FR180204 (10 μ M), as well as combined treatment with rapamycin (10 nM) and FR180204 (10 μ M). The results indicate an increased cell death of Nuc1 astrocytes after treatment with either rapamycin or FR180204. An additive effect was observed when both inhibitors were combined. —◆—, wt astrocyte with FR180204 treatment; —■—, wt astrocyte with rapamycin treatment; —▲—, wt astrocyte with rapamycin and FR180204 treatment; —×—, Nuc1 astrocyte with FR180204 treatment; —*—, Nuc1 astrocyte with rapamycin treatment; —○—, Nuc1 astrocyte with rapamycin and FR180204 treatment. For MTS (cell proliferation assay), the data represent the mean values of absorbance at wavelength 490 nm, which is proportional to the number of viable cells. For cell death assay, results were plotted as absorbance at 405 nm, with a reference wavelength of 490 nm. Experiments were performed in triplicate. *P*-values were calculated between Nuc1 and wt astrocytes by Student's *t*-test ($*P = 0.001$)

Primary culture of optic nerve astrocytes and anoikis induction. Optic nerve astrocytes from P2 wt and Nuc1 homozygous rats were cultured as described recently.²³ Cells were maintained in DMEM-F12 medium containing 10% FBS. To induce anoikis, 2.5×10^5 cells per well were seeded in six-well plates coated with poly-HEMA (Corning Inc., Corning, NY, USA). After 3 or 5 days of culture under low-attachment conditions, cells were analyzed or transferred to normal medium for later use. Photomicrographs were taken with an inverted microscope (Motic, Richmond, BC, Canada) at $\times 4$ magnification.

siRNA knockdown. siRNA duplex oligoribonucleotides for siRNA-targeted disruption of rat Bit1 (GenBank no. NM_001013860) were purchased from Dharmacon (Lafayette, CO, USA). A scrambled siRNA was also purchased from the same company and did not target any genes. Cultured astrocytes were transfected with 20 nM Bit1 or scrambled siRNA by using the Lipofectamine RNAiMAX reagent (Invitrogen, Carlsbad, CA, USA) according to the manufacturer's instruction. Knockdown of expression of Bit1 was verified by western blot analysis. Forty-eight hours after transfection, cells were seeded in six-well plates coated with poly-HEMA for further experiments.

Cell proliferation assay. Cell proliferation was determined by MTS colorimetric assay performed using 96-well plates (Promega, Madison, WI, USA)

following the manufacturer's protocol. Astrocytes were cultured under low-attachment conditions to induce anoikis for 5 days and were later seeded in CellTiter 96 cytotoxicity assay plates at 4×10^3 cells per well in 10% FBS medium. Cell numbers were determined at 0 and 7 days of incubation by adding 20 μ l of MTS solution to each well. After 1 h of incubation at 37 $^{\circ}$ C, absorbance, which is proportional to the number of viable cells, was measured at a wavelength of 490 nm. Experiments were performed in triplicate.

Cell death assay. Cell death evaluation by ELISA using the colorimetric Cell Death Detection ELISA^{PLUS} kit (Roche Applied Science, Indianapolis, IN, USA) was performed using 96-well strips according to the manufacturer's protocol. The relative amounts of mono- and oligonucleosomes generated from the apoptotic cells were quantified by using monoclonal antibodies directed against DNA and histones by ELISA. Briefly, wt and Nuc1 astrocytes were cultured under low-attachment conditions to induce anoikis for 3 and 5 days. The cytoplasmic fractions of wt and Nuc1 astrocytes were transferred onto a streptavidin-coated 96-well plate and incubated for 2 h at room temperature with a mixture of a peroxidase-conjugated anti-DNA and biotin-labeled anti-histone antibody. The plate was washed thoroughly, incubated with 2,2'-azino-di-(3-ethylbenzthiazoline sulfonate) diammonium salt and absorbance was measured at 405 nm, using a reference wavelength of 490 nm (DTX 880 Multimode Reader, Beckman Coulter Inc., Brea,

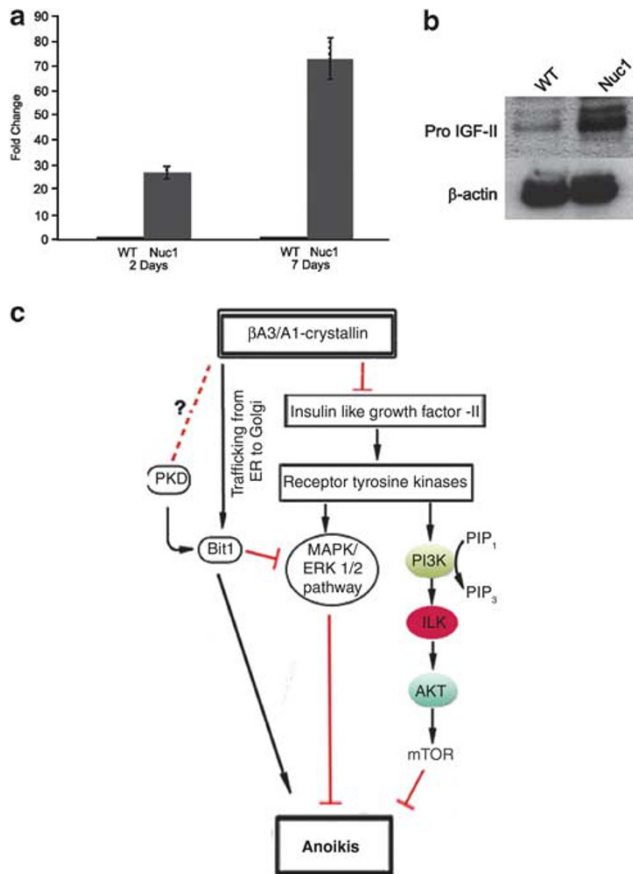


Figure 8 (a) Total RNA from 2- and 7-day cultures of wt and Nuc1 optic nerve astrocytes was assessed for reference (GAPDH) and target gene (IGF-II) by qRT-PCR. Fold change was calculated by the $\Delta\Delta C_T$ method after normalizing to GAPDH. Because of the small number of IGF transcripts in the wt sample, an arbitrary C_T value of 40 was assigned to the wt sample to measure fold change. (b) Western blot analysis for proIGF-II expression in a 7-day culture of wt and Nuc1 optic nerve astrocytes. The immunoreactive bands at ~20–21 kDa corresponding to the molecular weight of proIGF-II were upregulated in the Nuc1 astrocytes as compared with the wt astrocytes. β -Actin was used as a loading control. (c) A hypothetical model showing possible actions of β A3/A1-crystallin in the regulation of anoikis. For induction of anoikis, trafficking of Bit1 to the Golgi is essential, and our data suggest that β A3/A1-crystallin is required in this process. β A3/A1-crystallin may also regulate the balance between cell death and survival of astrocytes by inhibiting growth factors, such as IGF-II, which are upstream from the survival pathways PI3K/ILK/AKT/mTOR and ERK. Loss of this protein may inhibit anoikis not only by affecting trafficking of Bit1 to the Golgi, but also by activating PI3K/ERK-related survival signaling pathways through regulation of IGF-II, PKD and ILK expression

CA, USA). All conditions were repeated in triplicate in at least two independent experiments and results were evaluated by Student's *t*-test.

Immunofluorescence studies. Immunofluorescence was performed on frozen sections and retinal flat mounts or cultured astrocytes as described earlier.^{22,23} Briefly, samples were incubated in phosphate-buffered saline (PBS), containing 5% normal goat serum, for 30 min prior to being incubated overnight with primary antibodies at 4 °C; washed in PBS; incubated for 1 h at room temperature with secondary antibodies; and washed again with PBS. Sections were mounted with the DAKO fluorescent mounting medium (DAKO Corporation, Carpinteria, CA, USA). The primary polyclonal rabbit antibodies used were PKD (1 : 500; Abcam, Cambridge, MA, USA), Bit1 (1 : 500; Abcam), giantin (1 : 50; Abcam). The secondary antibodies used were goat anti-rabbit IgG conjugated with Cy3 (1 : 200; Jackson Immunoresearch, West Grove, PA, USA) for both PKD and Bit1, and

Alexa-Fluor-568 donkey anti-mouse IgG (Invitrogen) for giantin. Fluorescent digital images were acquired with a Leica 6000 fluorescent microscope (Leica Microsystems, Wetzlar, Germany). Retinal flat mounts were analyzed by Zeiss LSM 510 confocal microscope (Carl Zeiss Microimaging, LLC, Thornwood, NY, USA).

SDS-PAGE and western blot analysis. Lenses were dissected from wt and Nuc1 eyes by the posterior approach. Lens tissue was rinsed in PBS and homogenized in the Mammalian Protein Extraction Reagent (M-PER) (Thermo Fisher Scientific, Rockford, IL, USA) with 1% 0.5 M EDTA and 1% protease inhibitor cocktail (Sigma-Aldrich, St. Louis, MO, USA), and 1 mM EDTA. Samples were incubated at 4 °C for 30 min on an end-over-end shaker, followed by centrifugation at 13 000 × *g* for 15 min. Wt and Nuc1 astrocytes, after 3 and 7 days of anoikis induction, were lysed on ice for 30 min in RIPA buffer (50 mM NaCl, 100 mM Tris (pH 8.0), 1% Triton X-100, 1% deoxycholic acid, 0.1% SDS, 5 mM EDTA and 10 mM NaF, supplemented with 1 mM phenylmethylsulfonyl fluoride) and protease inhibitor mixture (Sigma-Aldrich). After centrifugation at 13 000 × *g* for 15 min, the supernatant was harvested as the total cellular protein extract. Protein quantification was performed by using the Quick Start Bradford Protein Assay (Bio-Rad Laboratories, Hercules, CA, USA). Approximately 25 μ g of protein from the supernatant was mixed with 2 × LDS sample buffer (Invitrogen) and then heated in a boiling water bath for 3 min. Each sample was loaded onto a 4–12% Bis-Tris Nu-PAGE gel and run with MES buffer (Invitrogen). For western blotting, proteins were transferred to nitrocellulose membrane (Invitrogen) for 90 min and then blocked with 3% bovine serum albumin (BSA) in Tris-buffered saline (TTBS, 0.1% Tween-20) overnight at 4 °C. Blots were incubated with antibodies to either Bit1, PKD (Abcam; at 1 : 1000 dilution); AIF (Santa Cruz Biotechnology, Santa Cruz, CA, USA; at 1 : 1000 dilution); caspase-3, total PI3K, AKT, p44/42 MAPK (Erk1/2), mTOR, phospho-PI3K (p85 (Tyr458)/p55 (Tyr199)), phospho-AKT (Ser473), phospho-p44/42 MAPK (Erk1/2) (Thr202/Tyr204), phospho-PKD (Ser916 and Ser744/748) and mTOR (Ser2448) (all from Cell Signaling Technology Inc., Danvers, MA, USA; all at 1 : 1000 dilution); or an anti-IGF-II antibody (clone S1F2, Millipore, Billerica, MA, USA; at 1 : 500 dilution). Blots were incubated with HRP-conjugated secondary antibodies (Kirkegaard and Perry Laboratories, Gaithersburg, MD, USA) for 1 h at room temperature at a dilution of 1 : 5000, followed by four washes of 10 min each. ECL western blotting detection reagents (GE Healthcare, Piscataway, NJ, USA) were used for detection with varying exposure times.

Real-time RT-PCR. Total RNA was extracted from wt and Nuc1 cells using the RNeasy Plus Mini Kit (Qiagen, Valencia, CA, USA) following the manufacturer's instructions and was quantified with a Nanodrop ND-1000 spectrophotometer (Thermo Scientific, Wilmington, DE, USA). A 2- μ g weight of total RNA was reverse-transcribed to cDNA in a 20- μ l reaction volume using the SuperScript reverse transcription kit (Invitrogen). Reverse transcription reaction was performed according to the manufacturer's instructions. PCR amplification was performed by using the 7500 PCR Fast Real-Time System (Applied Biosystems, Foster City, CA, USA) and custom-made TaqMan probes for IGF-II (Rn01454518_m1*) and GAPDH (Rn01775763_g1*). The reaction consisted of the following steps: enzyme activation at 95 °C for 20 s, 40 cycles of denaturation at 95 °C for 3 s, combined with annealing/extension at 60 °C for 30 s. All data were analyzed by using the ABI 7500 Real-Time PCR System, using the DataAssist software (Applied Biosystems), and graphs were plotted by using Microsoft Excel. All data are representative of experiments performed at least three times in triplicate. The data are represented as mean \pm S.D. For statistical analysis, Student's *t*-test was performed and a *P*-value of < 0.05 was considered statistically significant.

Conflict of Interest

The authors declare no conflict of interest.

Acknowledgements. This work was supported by grants from National Institutes of Health, EY018636 (DS), EY019037 (DS), EY019037-S (DS) and EY01765 (Wilmer Imaging Core); the Helena Rubinstein Foundation (DS) and Research to Prevent Blindness (an unrestricted grant to The Wilmer Eye Institute). We thank the staff members at Spring Valley Laboratories (Woodbine, MD, USA) for taking care of the experimental animals. We also thank Bhaja K Padhi, Eric Wawrousek, Gerard A Luty, James P Handa, Stanislav Tomarev, Morton F Goldberg and Nilkantha Sen for critically reading and discussions regarding the manuscript.

1. Kondoh H. Development of the eye In: J Roasant, P Tam (eds). *Mouse Development, Patterning, Morphogenesis, and Organogenesis*. Academic Press: San Diego, CA, USA, 2002, pp 519–538.
2. Wride MA. Lens fibre cell differentiation and organelle loss: many paths lead to clarity. *Philos Trans R Soc Lond B Biol Sci* 2011; **366**: 1219–1233.
3. Swaroop A, Kim D, Forrest D. Translational regulation of photoreceptor development and homeostasis in the mammalian retina. *Nat Rev Neurosci* 2010; **11**: 563–576.
4. Valenciano AI, Boya P, de la Rosa EJ. Early neural cell death: numbers and cues from the developing neuroretina. *Int J Dev Biol* 2009; **43**: 1515–1528.
5. Gilmore AP. Anioikis. *Cell Death Differ* 2005; **12**: 1473–1477.
6. Chiarugi P, Giannoni E. Anioikis: a necessary death program for anchorage-dependent cells. *Biochem Pharmacol* 2008; **76**: 1352–1364.
7. Biliran H, Jan Y, Chen R, Pasquale EB, Ruoslahti E. Protein kinase D is a positive regulator of Bit1 apoptotic function. *J Biol Chem* 2008; **283**: 28029–28037.
8. Jan Y, Matter M, Pai J-T, Chen Y-L, Pilch J, Komatsu M *et al*. A mitochondrial protein, Bit1, mediates apoptosis regulated by integrins and Groucho/TLE corepressors. *Cell* 2004; **116**: 751–762.
9. Yi P, Nguyen DC, Higa-Nishiyama A, Auguste P, Boucheccareilh M, Dominguez M *et al*. MAPK scaffolding by Bit1 in the Golgi complex modulates stress resistance. *J Cell Sci* 2010; **123**: 1060–1072.
10. Kairouz-Wahbe R, Biliran H, Luo X, Khor IW, Wankell M, Besch-Williford C *et al*. Anioikis effector Bit1 negatively regulates Erk activity. *Proc Natl Acad Sci USA* 2008; **105**: 1528–1532.
11. Frisch SM, Screaton RA. Anioikis mechanisms. *Curr Opin Cell Biol* 2001; **13**: 555–562.
12. Zhan M, Zhao H, Han ZC. Signalling mechanisms of anioikis. *Histol Histopathol* 2004; **19**: 973–983.
13. Danilkovitch A, Donley S, Skeel A, Leonard EJ. Two independent signaling pathways mediate the anti-apoptotic action of macrophage-stimulating protein on epithelial cells. *Mol Cell Biol* 2000; **20**: 2218–2227.
14. Kim J, Song G, Gao H, Farmer JL, Satterfield MC, Burghardt RC *et al*. Insulin-like growth factor II activates phosphatidylinositol 3-kinase-protooncogenic protein kinase 1 and mitogen-activated protein kinase cell signaling pathways, and stimulates migration of ovine trophectoderm cells. *Endocrinology* 2008; **149**: 3085–3094.
15. Singh SK, Moretta D, Almaguel F, De Leon D, De Leon DD. Precursor IGF-II (proIGF-II) and mature IGF-II (mIGF-II) induce Bcl-2 and Bcl-X_L expression through different signaling pathways in breast cancer cells. *Growth Factors* 2008; **26**: 92–103.
16. Bassnett S, Mataic D. Chromatin degradation in differentiating fiber cells of the eye lens. *J Cell Biol* 1997; **137**: 37–49.
17. Dahm R. Lens fibre differentiation—a link with apoptosis. *Ophthalm Res* 1999; **31**: 163–183.
18. Wride MA. Minireview: apoptosis as seen through a lens. *Apoptosis* 2000; **5**: 203–209.
19. Aarts HJ, Lubsen NH, Schoenmakers JG. Crystallin gene expression during rat lens development. *Eur J Biochem* 1989; **183**: 31–36.
20. Parthasarathy G, Ma B, Zhang C, Gongora C, Zigler Jr JS, Duncan MK *et al*. Expression of β A3/A1-crystallin in the developing and adult rat eye. *J Mol Histol* 2011; **42**: 59–69.
21. Sinha D, Hose S, Zhang C, Neal R, Ghosh M, O'Brien TP *et al*. A rat spontaneous mutation affects programmed cell death during the early development of the eye. *Exp Eye Res* 2005; **80**: 323–335.
22. Sinha D, Klise A, Sergeev Y, Hose S, Bhutto IA, Hackler Jr L *et al*. A3/A1-crystallin in astroglial cells regulates retinal vascular remodeling during development. *Mol Cell Neurosci* 2008; **37**: 85–95.
23. Zhang C, Asnaghi L, Gongora C, Patek B, Hose S, Ma B *et al*. A developmental defect in astrocytes inhibits programmed regression of the hyaloid vasculature in the mammalian eye. *Eur J Cell Biol* 2011; **90**: 440–448.
24. Turner DL, Cepko CL. A common progenitor for neurons and glia persists in rat retina late in development. *Nature* 1987; **328**: 131–136.
25. Turner DL, Snyder EY, Cepko CL. Lineage-independent determination of cell type in the embryonic mouse retina. *Neuron* 1990; **4**: 833–845.
26. Small RK, Riddle P, Noble M. Evidence for migration of oligodendrocyte-type-2 astrocyte progenitor cells into the developing rat optic nerve. *Nature* 1987; **328**: 155–157.
27. Barres BA, Hart IK, Coles HSR, Burne JF, Voyvodic JT, Richardson WD *et al*. Cell death and control of cell survival in the oligodendrocyte lineage. *Cell* 1992; **70**: 31–46.
28. Burne JF, Raff MC. Retinal ganglion cell axons drive the proliferation of astrocytes in the developing rodent optic nerve. *Neuron* 1997; **18**: 223–230.
29. Krueger B, Burne JF, Raff MC. Evidence for large-scale astrocyte death in the developing cerebellum. *J Neurosci* 1995; **15**: 3366–3374.
30. Zhang C, Gehlbach P, Gongora C, Cano M, Fariss R, Hose S. A potential role for β - and γ -crystallins in the vascular remodeling of the eye. *Dev Dyn* 2005; **234**: 36–47.
31. Gehlbach P, Hose S, Lei B, Zhang C, Cano M, Arora M *et al*. Developmental abnormalities in the Nuc1 rat retina: a spontaneous mutation that affects neuronal and vascular remodeling and retinal function. *Neuroscience* 2006; **137**: 447–461.
32. Kuszak JR. Development of sutures in the lens. *Prog Retinal Eye Res* 1995; **14**: 567–591.
33. Ruoslahti E, Reed J. Anchorage dependence, integrins, and apoptosis. *Cell* 1994; **74**: 477–478.
34. Martinou J-C, Dubois-Dauphin M, Staple JK, Rodriguez I, Frankowski H, Missotten M *et al*. Overexpression of bcl-2 in transgenic mice protects neurons from naturally occurring cell death and experimental ischemia. *Neuron* 1994; **13**: 1017–1030.
35. Burne J, Staple J, Raff M. Glial cells are increased proportionally in transgenic optic nerves with increased numbers of axons. *J Neurosci* 1996; **16**: 2064–2073.
36. Chan-Ling T, Chu Y, Baxter L, Weible II M, Hughes S. *In vivo* characterization of astrocyte precursor cells (APCs) and astrocytes in developing rat retinae: differentiation, proliferation and apoptosis. *Glia* 2009; **57**: 39–53.
37. Zigler Jr JS, Zhang C, Grebe R, Sehrawat G, Hackler Jr L, Adhya S *et al*. Mutation in the β A3/A1-crystallin gene impairs phagosome degradation in the retinal pigmented epithelium of the rat. *J Cell Sci* 2011; **124**: 523–531.
38. Attwell S, Roskelley C, Dedhar S. The integrin-linked kinase (ILK) suppresses anioikis. *Oncogene* 2000; **19**: 3811–3815.
39. Daniai NN, Korsmeyer SJ. Cell death: critical control points. *Cell* 2004; **116**: 205–219.
40. MacFarlane M. Cell death pathways – potential therapeutic targets. *Xenobiotica* 2009; **39**: 616–624.



Cell Death and Disease is an open-access journal published by Nature Publishing Group. This work is licensed under the Creative Commons Attribution-NonCommercial-No Derivative Works 3.0 Unported License. To view a copy of this license, visit <http://creativecommons.org/licenses/by-nc-nd/3.0/>